ENERGY DISTRIBUTION OF H⁻ IONS FROM THE ISIS ION SOURCE

D.C. Faircloth and J.W.G. Thomason, CCLRC, RAL, ISIS, Chilton, Didcot, Oxon, OX11 0QX, UK
M Haigh, I. Ho-ching Yiu, J. Morrison and G. Doucas, (Dept. of Physics, University of Oxford)

Abstract

We have used a specially designed retarding field energy analyzer with a resolution ($\Delta E/E$) of approximately 2×10^{-4} in order to measure the energy distribution, under different operating conditions, of the H^- beam of the ISIS ion source. The paper presents the details of the analyzer and the first results obtained on the Ion Source Test Facility at RAL.

INTRODUCTION

Analyser Construction

The energy analyser used is of the retarding field type - the beam is passed through a potential barrier, and the energy spectrum is deduced from measurements of the beam transmission as a function of barrier potential. The analyser (fig. 1) consists of several coaxial disc-shaped electrodes supported by ceramic posts, with apertures on the analyser axis to allow passage of the beam.

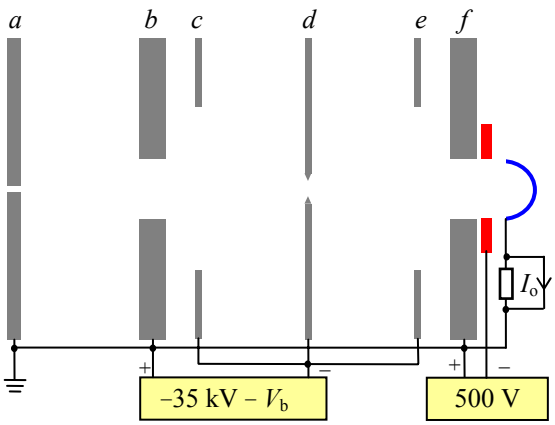

Figure 1: Schematic of the energy analyser, including electrodes (a-f, grey), suppressor (red) and Faraday cup (blue).

The electrodes *b*, *c*, *e*, and *f*, are positioned symmetrically on either side of the retarding electrode *d*, and form a lensing system. Electrodes *c*, *d* and *e* are connected to the negative terminal of a 300V bias supply, the positive terminal of which is connected to the HT platform. Ions enter the analyser with energies around the platform potential, so by changing the bias voltage then the potential at the retarding electrode can be varied over the range of ion energies, between complete transmission and complete attenuation of the beam.

Electrodes *b* and *c* focus the beam to a point in the centre of the aperture of *d*. This focusing is necessary because the retarding potential varies across the aperture, and so a dispersed beam of ions would see a large range of potentials; the resolution required of the analyser is thus only achievable by focusing the beam. Electrodes *e* and *f* recollimate the beam after it has passed through the retarding electrode, and allow the measurement apparatus to operate at ground potential.

The transmitted beam is collected on a Faraday cup placed after the last electrode, and the current on the cup is measured by a current preamplifier. A small suppression voltage deflects back any secondary electrons emitted from the cup. Electrode *a* restricts the amount of beam entering the analyser, so that it is not swamped.

The optimum geometry for the focusing and retarding electrodes in this type of analyser was calculated using SIMION modelling software.

The analyser has a finite resolution, since the energy which an ion must have to be transmitted through the analyser at a given potential, is a function of the angle at which it approaches the retarding electrode. This is because the proportion of an ion's energy associated with motion along the analyser axis is dependent upon its approach angle. This effect is parameterised by the instrument function $f\ (E + eV_b)$, which gives the proportion of ions with energies E in excess of the platform potential, which are transmitted through the analyser with the bias voltage set to V_b. This function was calculated in the 3D modelling work; it contains a significant offset because the magnitude of the potential in the centre of the retarding aperture is less than that on the electrode surface. The measured current I_o is given by:

$$I_o = -e\int_0^\infty f(E+eV_b)n(E)dE \qquad (1)$$

where $n(E)dE$ is the number of ions with energies in the range $(E,\ E+dE)$ passing through the analyser each second. The analyser is positioned to examine the core of the ion beam; the function $n(E)$ should therefore be proportional to the energy spectrum of this part of the beam. Equation (1) may be rewritten in terms of the resolution function $r\ (E+eV_b)$:

$$\frac{dI_o}{dV_b} = -e\int_0^\infty r(E+eV_b)n(E)dE \qquad (2)$$

Where: $r(E+eV_b) = \frac{d}{dV_b} f(E+eV_b)$.

Because the instrument function varies from unity to zero over only a few eV, equation (2) provides the most convenient means to deduce $n(E)$ from measured values of I_o.

CONTROL AND AUTOMATION

The 300V bias supply is controlled via a DC 0 to -5 V control voltage V_c. The computer sends a control string

from its serial port in RS-232 format; this is transmitted to the platform by fibre optic cables, and translated into a control voltage signal by a receiver circuit. The 300V bias supply is connected to the analyser by HT cable; the analyser potential is thus controlled from the computer.

The voltage signal from the analyser preamplifier, and also the voltage across a resistor connected to the toroid coil, are fed into a digital to analogue interface module (DAP) which communicates with the computer via an I/O card designed for the purpose. A program written in the DAPL language instructs the interface to trigger a data collection pulse on reading a sufficient current from the toroid; instances of this program are invoked from the main control program written in C++, which also sweeps the analyser through a range of voltages, and processes the collected data. The mean analyser signal, along with other characteristics, is calculated for each pulse, and the overall statistics for all the pulses taken at a given voltage are also calculated. The data is saved in a text format amenable to further analysis by spreadsheet or graphing packages.

RESULTS

The results presented here are those obtained under normal conditions and also at different levels of source discharge current. Transmission curves were built up with data at voltage intervals of 2 V, reading 10 pulses per voltage setting. The discrete differentials (i.e. differences between adjacent points) of the curves were plotted. Large artificial spikes due to source breakdowns were removed from the plots by a simple interpolation process. Equation (2) is a relation appropriate to continuous differential functions, but discrete differential data can be analysed by considering that if the sampling rate is much better than the scale of the distribution (as here), (2) can be written as a sum using discrete functions:

$$\frac{\delta I_o}{\delta V_b} = -e\sum_{E=0}^{\infty} r_{E+eV_b} n_E \qquad (3)$$

where r and n are the discrete equivalents of their counterparts in (2), δI_o is the discrete differential of the transmission curve, and δV_b is the sampling rate.

How equation (3) is used to interpret the measured data depends on the instrument resolution function. The resolution function calculated from modelling work on the analyser is a top hat function of width 5.4 eV centred at V_b = −124.4 V. The calculation was for a platform potential of −30 kV so while running at −35 kV a proportionately higher offset of V_b = −145.1 V is expected, since the potential drop across the retarding aperture will be increased.

The calculated resolution function is much narrower than the observed distributions of δI_o. It therefore seems reasonable to equate the δI_o distributions, corrected for the offset of the resolution function, with the actual energy spectra of the source. It is important to stress, however, that unquantifiable sources of resolution loss may make the distributions substantially wider than the real spectra; this is discussed later.

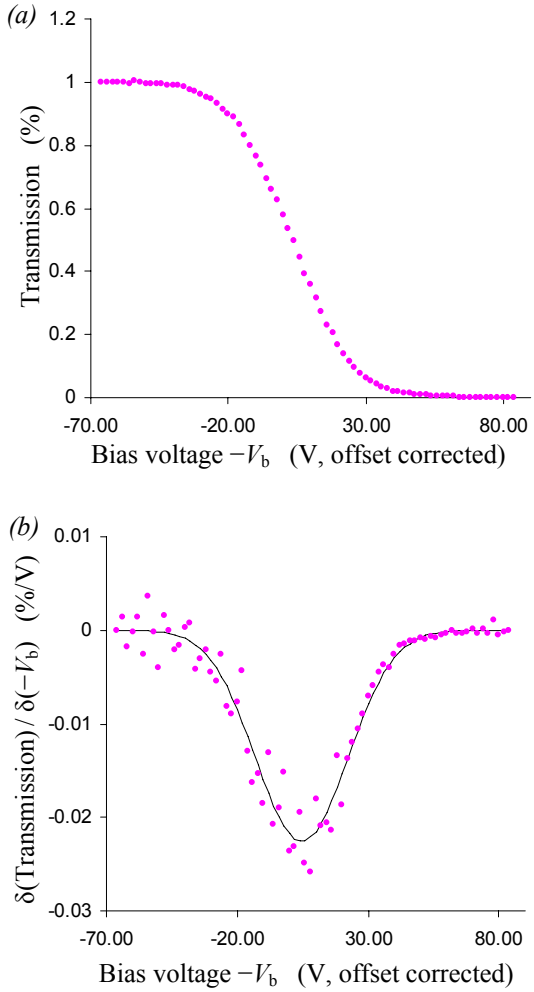

Figure 2: a) Transmission data for the ion source under normal operating conditions. b) The discrete differential of the data, with a Gaussian curve fitted.

The measured transmission curve (averaged over ten sets of data) for normal source operating conditions is shown in fig. 2, along with the resulting differential data with a Gaussian curve fitted. The measured transmitted currents have been scaled to a percentage of the maximum.

The lower energy part of the data shows significant statistical variability because the overall signal is larger in this region, but the measured distribution fits to a Gaussian curve rather well. The shown fit curve has width σ = 17.6 V ± 0.5 V, and is centred on μ = 4.6 V ± 0.5 V, where the errors quoted are those associated with curve fitting. The total source output current varied between the sets of readings from about 40 mA to 60 mA; the output shows random changes within this range over a timescale of hours, as well as sharper changes over a timescale of minutes. The effect does not appear to be systematic and

the energy spectrum is stable under the changes, but fluctuations in source behaviour within a spectrum measurement rendered many sets of data unusable.

Spectrum measurements were taken for discharge currents across the source in the range 40-95 A, c.f. the usual value of 50 A. Outside this range the source was too unstable to take any data. The other source parameters were held at normal values, but air cooling to the source was altered in order to control temperature changes. The data for these conditions is rather noisier than for normal operation and so the curve fitting errors are larger.

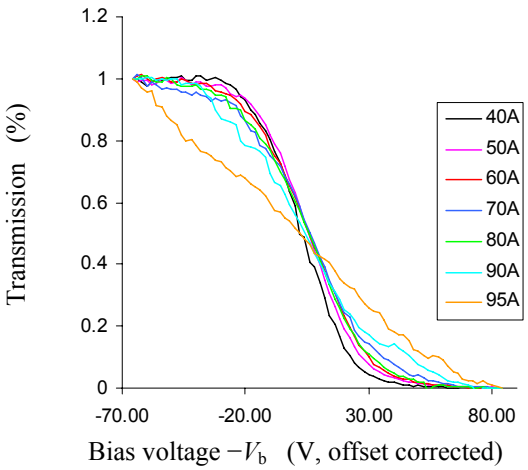

Figure 3: Transmission data for the ion source under varying discharge currents. Data is shown as lines rather than points for clarity.

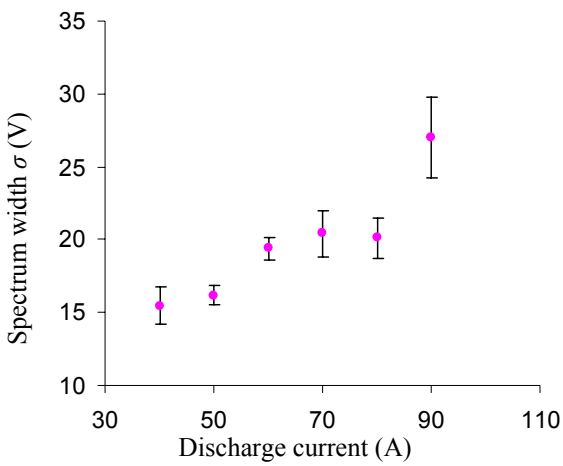

Figure 4: Widths for the source energy spectrum at different levels of discharge current. Error bars represent curve fitting errors.

Gaussian curves were fitted to the discrete differentials of the data; these are shown along with the raw transmission curves, and a plot showing the trend in spectral width, in Fig. 3. It can be seen that the energy spectrum grows considerably wider as the discharge current is increased. fig. 4. The distribution for 95 A, the highest value (not shown), is very wide and probably more like a top hat than a Gaussian. Little or no systematic change in the total beam current was observed by changing the discharge current.

DISCUSSION

The energy spectrum of the source appears to be much wider than the ~ 1 eV suggested by general literature on this type of source [1], and the reason for this is unclear. A possible explanation is that the source geometry does not completely inhibit the direct extraction of fast surface produced ions, as opposed to slow ions produced by charge exchange. One may expect (as is seen for some different source geometries) that the centre of the energy distribution would be at a point considerably greater than zero if this were true. However, it may be that the energy of negative ions upon leaving the cathode sheath is not, on average, associated with net motion along the beam direction. In this case one would expect the presence of fast ions in the extracted beam to produce a large spread in the energy spectrum, but no shift.

The calculated resolution function takes account only of effects due to the angular spread of the beam at the retarding electrode. Another problem is that the mutual repulsion of the ions in the beam will have a dispersing effect, leading to a finite beam width at the retarding electrode. This space charge effect is greatly exacerbated by the fact that the ions are decelerated and so move slowly near the retarding electrode, making small repulsive forces more important. The beam current passing through the analyser is about 2 μA, which could conceivably be enough to cause significant dispersal in a decelerated beam, but the effect would be difficult to quantify without further modelling work. Tolerances in the machining of the analyser will also limit resolution to an unknown degree.

CONCLUSION

The spectrum, as measured for normal source operation, is a Gaussian of width σ = 17.6 V ± 0.5, and this width is seen to increase significantly as the source discharge current is increased.

REFERENCES

[1] J Peters, “Review of Negative Hydrogen Ion Sources High Brightness/High Current”, Proceedings, Linac 98 conference.

[2] M Haigh “PP5: High performance H− ion source”, Final Year Project, Oxford University 2006.